



ANNUAL REVIEWS **Further**

Click [here](#) to view this article's
online features:

- Download figures as PPT slides
- Navigate linked references
- Download citations
- Explore related articles
- Search keywords

Image Formation in the Living Human Eye

Pablo Artal

Laboratorio de Óptica, Instituto Universitario de investigación en Óptica y Nanofísica,
Universidad de Murcia, E-30100 Murcia, Spain; email: pablo@um.es

Annu. Rev. Vis. Sci. 2015. 1:1–17

First published online as a Review in Advance on
July 22, 2015

The *Annual Review of Vision Science* is online at
vision.annualreviews.org

This article's doi:
10.1146/annurev-vision-082114-035905

Copyright © 2015 by Annual Reviews.
All rights reserved

Keywords

optics, retinal image, aberrations, intraocular scatter, spatial vision

Abstract

The human eye is a relatively simple optical instrument that imposes the first performance limits on the visual system. This review describes the main optical properties of the eye: geometric image formation, aberrations, and intraocular scattering. The article also discusses the sources of optical degradations and their impact on visual performance.

INTRODUCTION

Considered as an optical instrument, the human eye is rather simple. It is formed by only two positive lenses, the cornea and the crystalline lens, that combine to project images of a scene onto the photoreceptor layer of the retina. Thus, although the eye is less complex than many artificial optical systems, which often comprise many lenses, this simple structure is well adapted to the requirements of the visual system: the formation of good quality images of objects placed at different distances over a large field of view.

Although the optical part of the eye is arguably the simplest one of the visual system, this part plays a crucial role in it. The nature of the light and the properties of the eye combine to impose a first physical limit to vision that cannot be avoided. If the retinal images are blurred, the visual system will not function properly, and vision will be poor. The opposite is not true, however; many retinal and neural diseases impair vision even when good quality retinal images are formed. This article aims to provide a general overview of the image formation properties of the eye and to show how these properties may limit the performance of the visual system.

NATURE OF LIGHT AND IMAGE FORMATION

The fundamental physical limit to vision results from the nature of light. The eye is adapted to the visible part of the spectrum in both its ability to transmit light and its sensitivity to perceive it. Under most visual conditions, light may be considered as a transverse electromagnetic wave. Light waves of a single color (monochromatic waves) have electric fields with sinusoidal oscillation in a direction perpendicular to that of their traveling paths. A sinusoidal magnetic field also oscillates in a plane perpendicular to the electric field. The wavelength of light is given by the distance between two consecutive maxima of these oscillations. Visible light falls within a very small (300-nm) fraction of the electromagnetic spectrum—its wavelengths range from approximately 400 nm (blue) to 700 nm (red)—and its wavelike nature explains properties that may impact vision such as interference, polarization, and diffraction. Although an even a simpler description, light as rays pointing along the direction of wave propagation, is valid to approximate the image properties of the eye, the wave character of light (Pedrotti & Pedrotti 1993) and the consequences of this character cannot be ignored in many practical conditions.

A few phenomena, such as the absorption of light by matter, can be interpreted only if light is considered a particle, called a photon. Photon absorptions occur in the photoreceptors of the eye following the rules of a random process; absorptions occur discontinuously and in discrete quanta. Specifically, the light intensity reaching each photoreceptor determines only the probability of a photon being absorbed, imposing another fundamental limit to vision that is related to the photon statistics of the retinal image (Pelli 1990). The impact of this randomness is limited to very low luminance conditions after dark adaptation. In this review, I consider only those visual situations in which quantum effects are not important and retinal image quality is governed by the wavelike nature of light.

The image forming properties of the eye are well described by Fourier optics (Goodman 2005); **Figure 1** shows schematically the main functions that characterize it. The wave aberration function is defined as the difference between the perfect (spherical) and real wavefront for every point over the pupil. This difference is commonly represented as a two-dimensional map in which each gray or color level represents the amount of wave aberration, expressed either in micrometers or as a number of wavelengths. The image of a point source, called a point spread function (PSF), can be computed as the Fourier transform of the complex pupil function, a function in which the phase is the wavefront aberration, and the modulus is the transmission over the pupil. An eye

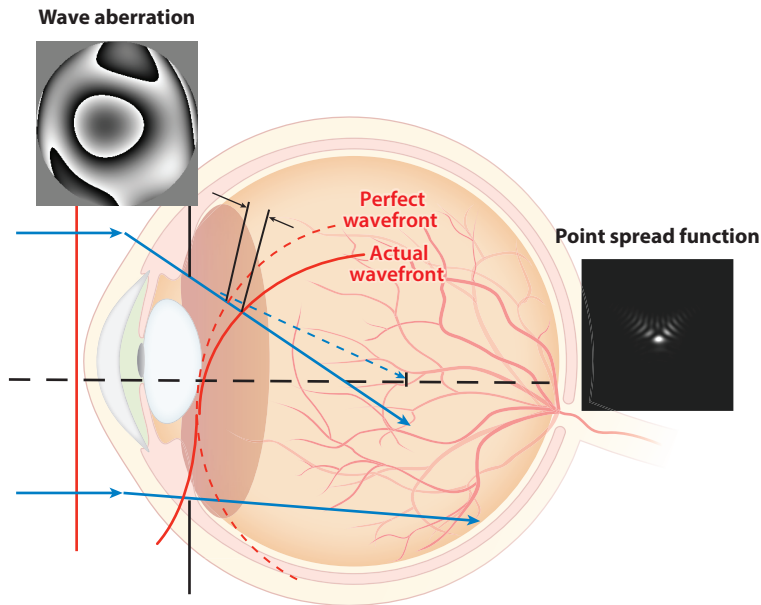


Figure 1

Functions used to describe the image quality of the eye. The wave aberration function is defined as the difference between the perfect (spherical) and the real wavefront for every point over the pupil. The image of a point source formed on the retina is called a point spread function (PSF).

without aberrations has a constant, or null, wave aberration and forms a perfect retinal image of a point source (called an Airy disc) that depends on only the pupil diameter. In contrast, an eye with aberrations produces a more extended, and generally asymmetric, retinal image (**Figure 2**). Although the wave aberration can be a complicated two-dimensional function, it can be expressed as the weighted sum of polynomials called aberration modes. For a given set of aberration modes,

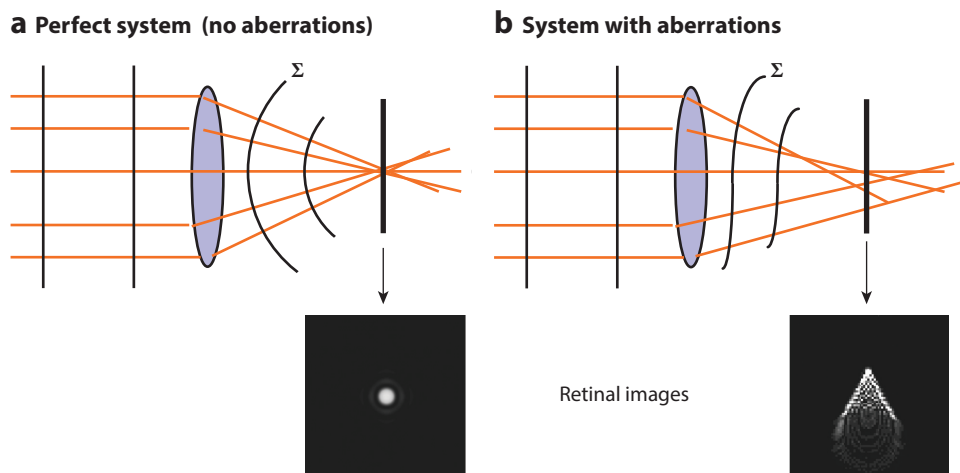


Figure 2

Examples of image formation in (a) a diffraction-limited eye and (b) an eye affected by aberrations.

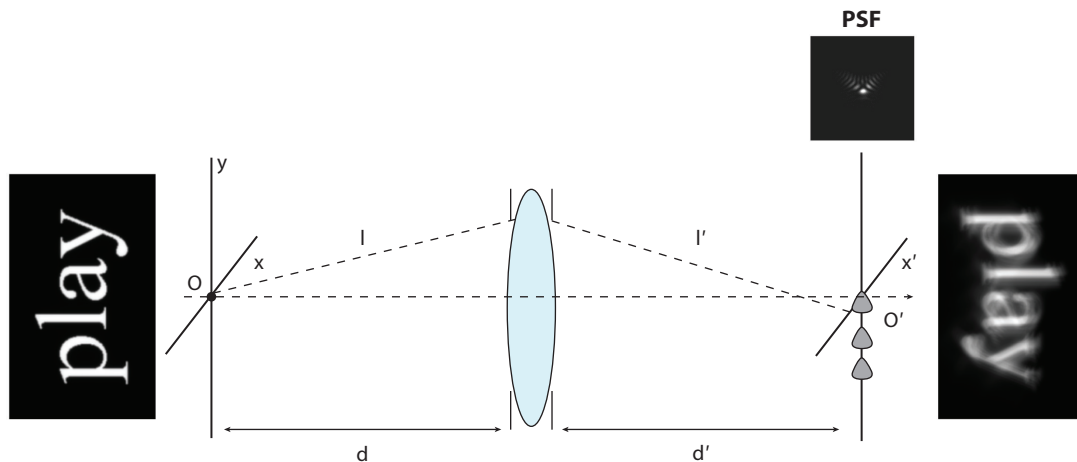


Figure 3

Schematic showing the formation of an extended image in the eye. The left side of the figure depicts object space, and the right side depicts image space. A weighted point spread function (PSF) convolved with each point of the geometrical image produces the simulated retinal image (*right*).

the lower-order polynomials correspond to defocus and astigmatism, and subsequent polynomials describe higher-order aberrations such as coma, spherical aberration, and triangular astigmatism, among others. The Zernike polynomials are a convenient set; these polynomials are defined on the unit circle and often used to decompose the wave aberration. A useful image quality parameter, the Strehl ratio, can be calculated as the quotient between the intensity peak of the PSF of an eye and that of the aberration-free (diffraction-limited) PSF. In addition, one can predict the retinal image of any object by performing a convolution operation (**Figure 3**). This practice can be easily understood as placing a weighted PSF onto each point of the geometric image.

Several factors are responsible for the degradation of retinal images: diffraction of light in the pupil of the eye, optical aberrations (chromatic and monochromatic), and intraocular scattering. Diffraction blurs the images formed through instruments with a limited aperture owing to the wave nature of the light. The effect of diffraction in the eye is visually significant only when the pupil diameter is less than 2 mm.

OPTICAL PROPERTIES OF THE EYE

The adult human eye resembles a sphere with a diameter of approximately 24 mm. Light entering the eye is first refracted by the cornea, a thin transparent layer free of blood vessels that is approximately 12 mm in diameter and the center of which is approximately 0.55 mm thick. An aqueous tear film on the cornea ensures that the first optical surface is smooth, thereby providing the best image quality. Behind the cornea lies the anterior chamber, which is filled with the aqueous humor. The iris, a sphincter muscle with a central hole whose size depends on the level of muscular contraction, acts as a diaphragm. The pupil is the variable opening in the center of the iris, which controls retinal illumination and limits the rays of light entering into the eye. The pupil size changes with the amount of ambient light; it varies from less than 2 mm in diameter in bright light to more than 8 mm in the dark. Thus, the pupil affects the retinal image quality. Once light has passed through the iris, the crystalline lens works together with the cornea to form the retinal image. The crystalline lens changes shape to modify its own optical power and therefore that of

the whole eye. This modification is the basis of the mechanism of accommodation, which allows the eye to focus images on the retina. Objects in scenes may be placed at many different distances, from distant to near. After the light is refracted by the lens, it enters the posterior chamber, which is filled with the transparent vitreous humor, and reaches the retina. The human retina has a central area called the fovea, in which photoreceptors are densely packed to provide the highest resolution. The eyes move continuously to fixate the desired details on the fovea. The peripheral parts of the retina have lower resolution than the fovea, but they are important because they are specialized in movement detection and are needed to locate objects in the visual field.

The cornea is approximately a spherical section with an anterior radius of 7.8 mm, a posterior radius of 6.5 mm, and a refractive index of 1.3771. The largest difference in refractive index occurs from the air to the cornea (more specifically, the tear film overlying the cornea), accounting for most of the refractive power of the eye (on average over 70%). The lens is a biconvex lens with radii of 10.2 and -6 mm for the anterior and posterior surfaces, respectively. The internal structure of the lens is layered, producing a nonhomogeneous refractive index that is larger in the center than in the periphery and that has a mean value of 1.42. The refractive indexes of the aqueous and vitreous humors are 1.3374 and 1.336, respectively. An average eye with dimensions of 3.05, 4.0, and 16.6 mm for the anterior chamber, lens, and posterior chamber, respectively, will have an axial length of 24.2 mm and will image distant objects precisely in focus on the retinal photoreceptors by simple application of geometric optics principles. Most eyes have neither adequate optical properties nor the correct dimensions to achieve perfect focus, however; instead, they are affected by refractive errors. In these cases, the images formed on the retina are blurred, typically imposing a resolution limit to visual perception. Even in eyes free of any refractive error such as defocus or astigmatism, the optics do not produce perfect images. The retinal image of a point source is not another point; rather, it is an extended distribution of light, owing to a combination of optical aberrations, diffraction, and scattering.

The eye is not a centered optical system because the ocular surfaces are not spherical in shape and not perfectly aligned. In addition, the fovea is decentered temporally (by approximately 5° on average), and the lens can also be tilted and/or decentered with respect to the cornea. Thus, several key axes and angles are defined within the eye (Le Grand & El Hage 1980); these are represented schematically in **Figure 4**. The pupillary axis is the line perpendicular to the cornea that intersects the center of the entrance pupil. The line of sight connects the fixation point to the center of the entrance pupil (this line also connects the fovea with the center of the exit pupil). These axes may be considered approximations to the optical axis (pupillary axis) and the visual axis (line of sight)

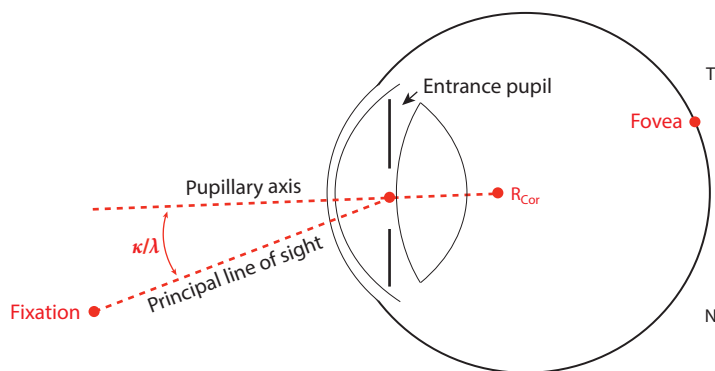


Figure 4

Schematic representation of the main axes and angles in the eye. Abbreviations: N, nasal; T, temporal.

of the eye (the visual axis connects the fixation point to the fovea via the nodal points). The angle kappa (κ) is the angular distance (in object space) between the line of sight and the pupillary axis.

Simple paraxial calculations applied in schematic eye models are used to predict important ocular properties including surface reflections such as Purkinje images, cardinal point locations, entrance and exit pupils, retinal illumination, and retinal size magnification (Atchison & Smith 2000). Geometrical optics is useful in many cases, such as to predict the approximate required power of intraocular lenses, but it is not sufficient to actually determine the optical quality of the retinal image.

The ocular media act as a band-pass filter that reduces the range of wavelengths reaching the retina. Overall, transmitted wavelengths are well matched to photoreceptor sensitivity, although the wavelengths of some light reaching the retina are too long to be detected. The cornea and the vitreous humor have transmission bandwidths that exceed the visible spectrum, but the lens absorbs light in the short-wavelength (blue) part of the visible light spectrum. Blue light absorption mitigates chromatic aberration and strongly increases with age (van Norren & Vos 1974). The retina also has pigments that filter the light reaching the photoreceptors. The main filter in the retina is the yellow macular pigment, which is located within the macular region near the fovea. The amount of macular pigment differs among individuals; its optical density ranges from 0.17 to 1.39 for 460-nm light (Hammond et al. 1997).

CHROMATIC ABERRATIONS

Chromatic aberrations arise from the dependence of refractive index on wavelength. This dependence means that objects of different colors are imaged onto the retina at different locations. There are two types of chromatic effects in the retinal image: longitudinal chromatic aberration (LCA), the variation of power with wavelength, and transverse chromatic aberration (TCA), the shift of the image position in the retina for different wavelengths. Because the eye is a waterlike sphere, both types of aberration have a significant presence and limit the retinal image quality of white-light scenes. LCA has been measured and modeled extensively for many decades (Wald & Griffin 1947). The studies consisted of measuring the subjective best focus for each color (Bedford & Wyszecki 1957) or the objective best focus using retinoscopic methods (Charman & Jennings 1976) or wavefront sensors (Manzanera et al. 2008). Consistently across studies, subjects, and age (Howarth et al. 1988), the LCA has been found to be around 2 diopters (D) for the visual spectrum. **Figure 5a** shows the typical LCA predicted with a simple water-eye model (Thibos et al. 1992), which agrees well with experimental measurements (Manzanera et al. 2008).

TCA has been measured psychophysically using vernier alignment tasks for two colors (blue and red) in a Maxwellian view system (Simonet & Campbell 1990) or with a pinhole pupil (Thibos et al. 1990). The perceived TCA has been measured under normal viewing conditions with the complete pupil, and it represents the mean apparent prism differences across the pupil. In contrast to the LCA, the TCA varies widely among studies and subjects both in magnitude and direction. A centered system should not present TCA on-axis, so ocular TCA is usually assumed to arise from the off-axis position of the fovea and from natural pupil misalignments. A recent study showed that in most subjects, the achromatic axis is located near the first Purkinje reflex (Manzanera et al. 2015). **Figure 5b** shows example retinal images of three letters in both monochromatic (left panel) and polychromatic light (right panel). The white-light image was obtained including the effects of both LCA and TCA. Despite the apparent color degradation in the retinal image, the real visual impact of chromatic aberration is relatively small. There are several explanations for this fact: The relatively strong filtering of blue light in the lens and macular pigment and the heightened sensitivity to longer wavelengths reduce the contribution of the most defocused bluish colors.

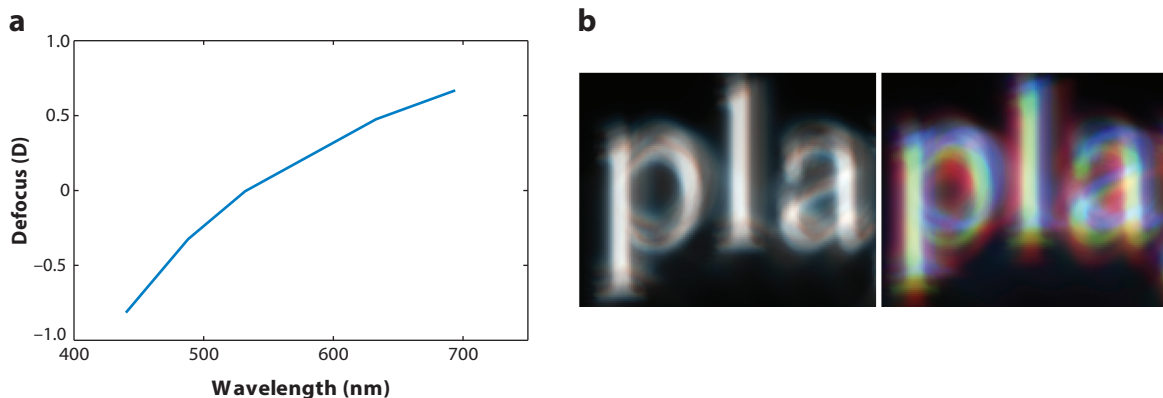


Figure 5

(a) Typical longitudinal chromatic aberration (LCA). (b) Example retinal images of three letters in monochromatic (*left*) and polychromatic (*right*) light. The calculation used to create these images included both LCA and transverse chromatic aberration (TCA).

During the past several decades, many researchers have sought to correct chromatic aberrations using achromatizing lenses (Powell 1981, Benny et al. 2007). However, chromatic correction is sensitive to centration errors because small displacements of either the correcting lens or the eye result in additional TCA that degrades image quality (Zhang et al. 1991), so a misalignment of just 0.4 mm is enough to eliminate the potential benefit of achromatization. For larger displacements, the achromatizing lens actually worsens image quality. A practical alternative is the use of chromatic diffractive correctors (Díaz et al. 2004), which can be implemented in, for example, intraocular lenses. To better understand the impact of chromatic aberrations in vision we used an adaptive optics instrument to evaluate the effect of correcting both LCA and spherical aberration (SA) (Artal et al. 2010). The correction of SA alone had a larger impact on contrast vision than did correction of LCA. Chromatic and spherical aberration depend differently on the pupil diameter: SA depends on the fourth power of the radius, whereas LCA depends on the squared radius. Thus, the benefit of the correction depends on pupil size. The impact of chromatic aberration in binocular visual acuity has also been studied recently (Schwarz et al. 2014). Although correction of SA had a greater impact monocularly than binocularly in monochromatic light, bilateral correction of both SA and LCA may further improve binocular spatial visual acuity. If so, this finding may support the use of aspheric-achromatic ophthalmic devices to improve vision.

MONOCHROMATIC ABERRATIONS

Monochromatic aberrations in the eye depend on many factors and conditions such as pupil size (Artal & Navarro 1994), age (Artal et al. 1993), accommodation (He et al. 2000), retinal eccentricity (Jaeken & Artal 2012), and possible corneal (Vinciguerra et al. 2009) or lenticular pathologies (Kuroda et al. 2002) that are beyond the scope of this review.

As in any optical system, ocular aberrations increase for large pupil diameters. As the normal pupil diameter in the eye ranges from 2 to 8 mm, its aperture values (f-numbers) range from f/8 to f/2, which can be compared with those typically found in a camera objective (a 35-mm camera lens typically has an aperture range of f/2 to f/22). Aberrations for an eye with an aperture of roughly f/4 have a magnitude approximately equivalent to less than 0.25 diopters of defocus. For this situation (a pupil diameter of approximately 5 mm), the root mean square (RMS) of the wave

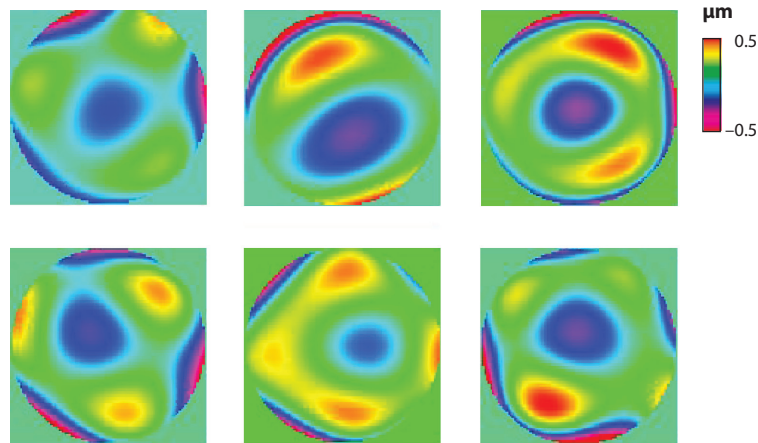


Figure 6

Examples of wave aberrations for different normal healthy eyes: Each eye shows a specific and unique set of spatial features.

aberration is approximately $0.25 \mu\text{m}$. Each eye has a unique aberration pattern (see **Figure 6** for examples of wave aberrations from different eyes, each showing specific spatial features).

Normal eyes have relatively poor image quality compared with that of artificial optical systems. A common criterion used in instrumental optics was introduced by Maréchal (1947) and states that an optical system is well corrected only when its wavefront error is smaller than $\lambda/14$, where λ is the wavelength of the light passing through the system. A normal human eye exceeds this value by sixfold, justifying the assessment of the human eye as having low-quality optics. Under normal conditions, however, aberrations do not impose a limit to vision; rather, the lower-order aberrations, defocus and astigmatism, are the main sources of degradation in the retinal image. A small amount of defocus (roughly $\pm 0.25 \text{ D}$) has a relatively small impact on visual acuity, but larger values of defocus cause visual acuity to drop quickly. Similarly, small amounts of natural astigmatism ($< 0.5 \text{ D}$) have only a small impact on visual acuity (Villegas et al. 2014). The reason for this tolerance is the coupling of lower-order aberrations with both higher-order aberrations and retinal and neural limits.

There is a significant tendency toward reduced visual acuity as aberrations increase beyond the normal value of $0.25 \mu\text{m}$. However, the impact of normal amounts of aberrations ($\leq 0.25 \mu\text{m}$) is not as clear. There are at least three possible descriptions of the relationship between the magnitude of aberrations in the human eye and its visual acuity. One suggests that the lower the amount of aberrations in an eye, the better its visual performance. In such a situation, an aberration-free eye (in which resolution is limited only by diffraction) would produce the highest visual acuity. A different option suggests that a specific type and/or nonzero magnitude of aberrations produces the best performance. A third possibility is that the particular aberrations of each person, provided they are within a normal range, produce the best visual acuity.

To understand how aberrations impact spatial vision, we measured the visual acuity and aberrations of the eyes of a group of normal young subjects under carefully controlled conditions (Villegas et al. 2008). We found that the measured amounts of aberrations among different subjects (expressed as RMS values) were not correlated with their visual acuities (**Figure 7**). Moreover, the subjects with the highest acuities did not always have the lowest amounts of aberrations. This finding suggests that having a normal pattern of aberrations provides the best visual performance

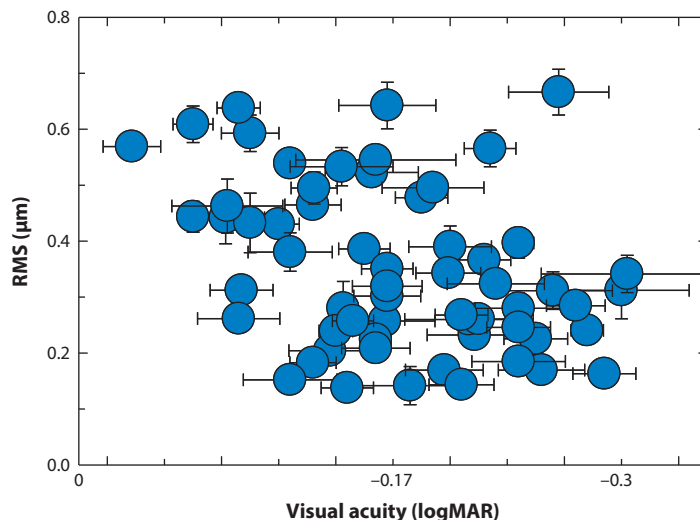


Figure 7

Plot showing amounts of aberrations [expressed as the root mean square (RMS)] versus logMAR (minimum angle of resolution) visual acuity in a group of normal subjects.

and supports the idea of a neural adaptation mechanism that compensates for the aberrations (Artal et al. 2004). If subjects adapt to their own specific aberration patterns, it is quite reasonable that the amount of aberrations would have a smaller effect on vision. Although the effect of neural adaptation is probably relatively small, such adaptation may contribute to the robustness of the visual system, leading to similar performance over a large range of ocular optics qualities.

Although the eye has a relatively low optical quality, the optical system itself is optimized. The two main optical components, the cornea and lens, have particular features that combine to improve the optical quality of the system. There is a long history of efforts to understand the relative optical contribution of the cornea and lens to the imaging properties of the eye as a whole. As early as 1801, Thomas Young (Young 1801) in a pioneering experiment neutralized the cornea by immersing his own eye in water and found that his astigmatism persisted. Today, it is commonly accepted that the lens compensates for moderate amounts of corneal astigmatism, spherical aberration, and coma. **Figure 8** shows wavefront aberrations for the right eye of the author for the anterior cornea, internal optics (mostly the lens), and the complete eye. A simple inspection of these wavefront maps indicates the role of the lens in partially compensating for some of the corneal aberrations. In addition to the spherical aberration, the horizontal corneal coma was mostly compensated by the crystalline lens (Artal et al. 2001, 2006; Tabernero et al. 2007; Artal & Tabernero 2008, Berrio et al. 2010). The compensation for horizontal coma is linearly related to the angle κ of the eye, which tends to be larger for hyperopic subjects than for myopic ones. The larger the angle κ , the larger both the corneal coma and the lens coma will be, although their signs will be opposite. **Figure 9** shows an example of this behavior in a group of eyes. The comas measured for both the cornea and the lens are represented as a function of the measured angle κ in each eye (Tabernero et al. 2006). This result indicates that the eye has a certain optical mechanism that makes it relatively insensitive to the presence of naturally occurring field angles such as the angle κ . A combination of a particular curvature, asphericity, and gradient index generates the negative spherical aberration in the lens required to partially balance the cornea. The cornea and the crystalline lens generate coma aberrations with opposite signs in the presence of a

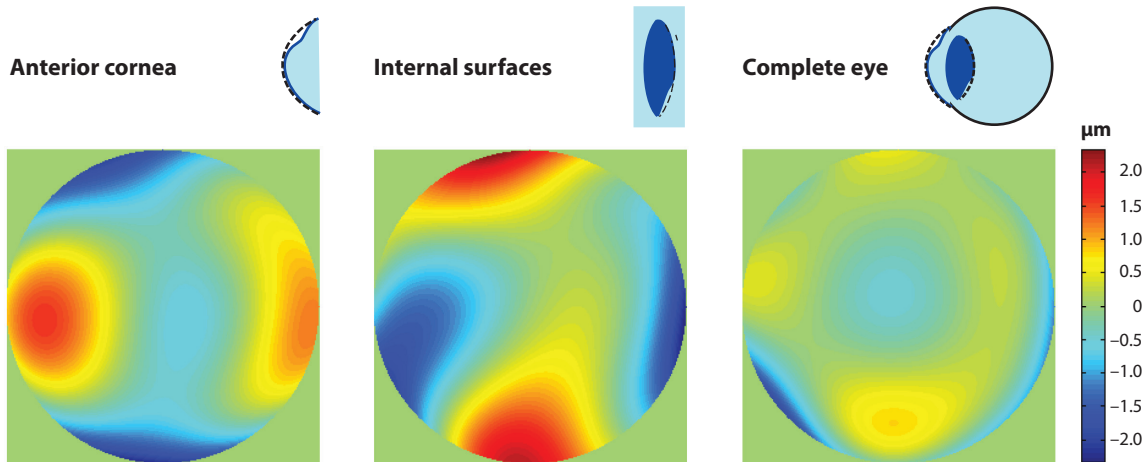


Figure 8

Examples of wavefront aberrations for the right eye of the author for the anterior cornea, internal optics (lens), and complete eye. Taken together, these plots are a graphical demonstration of the way in which the lens partially compensates for corneal aberrations.

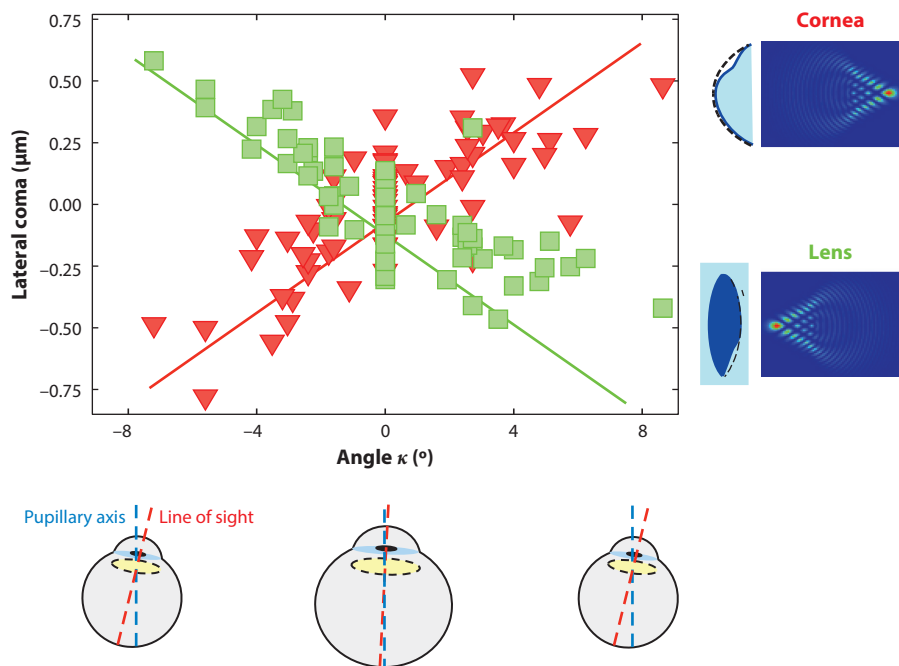


Figure 9

Coma values associated with the cornea and the lens in a group of subjects as a function of angle κ . The larger the angle is, the larger the coma for both the cornea and the lens. Note, however, that the coma values of the cornea and lens have opposite signs.

field angle. The corresponding values of coma for the shape factors of the cornea (approximately 1.2) and the lens (approximately -0.25) also have opposite signs. If the angle increases, coma increases as well, but the signs remain opposite the lens and the cornea. This special aplanatic design of the eye allows it to maintain a rather stable optical quality, independent of some ocular alignment variables. Nature probably imposed some limitations on the alignment design for the eye, but, to some degree, the shapes of the two lenses are, from an optical point of view, optimized.

An important detail is how the coupling between the aberrations of the cornea and those of the lens evolves during normal aging. The aberrations of the eye tend to increase with age, mainly owing to a disruption in this coupling. The cornea remains relatively stable, and the lens aberrations change with no coupled corneal change (Artal et al. 2002).

IMAGE QUALITY IN THE PERIPHERAL RETINA

Although more attention is usually given to the central visual field, which has the highest spatial resolution of our visual system, the periphery of the retina also plays a crucial role in it. In addition, the optics of the eye have completely different behavior when images are formed eccentrically. The oblique incidence of light on the eye produces off-axis (oblique or peripheral) aberrations that increase with the angle of eccentricity, causing the off-axis optical performance of the eye to deteriorate as one moves away from the center of the fovea. Moreover, the ability to discriminate small objects decreases severely with increasing eccentricity. For example, the normal resolution in the fovea is 1 minute of arc, whereas the resolutions at 10, 20, and 30° of eccentricity are 2.5, 5, and 10 minutes of arc, respectively. This increase may result from both optical and neural factors: The eccentric angle induces optical aberrations, which lower the contrast of the retinal image, and the density of cones and ganglion cells also declines with increasing eccentricity, resulting in sparse sampling of the image. Thus, although in many cases the optics of the eye can be the main limiting factor for central vision, vision in the periphery is limited by neural functionality. For example, gratings in the periphery can be detected even when their orientation cannot be identified, indicating that resolution acuity in the periphery is worse than detection acuity. This difference is a result of aliasing, a term used to describe the phenomenon in which a coarse neural sampling density misinterprets spatial frequencies above the Nyquist criterion as being lower, distorted frequencies (Artal et al. 1995).

The optics of any optical instrument are degraded for eccentric angles. For a spherical refracting surface, the Seidel off-axis aberrations are distortion (tilt), field curvature, astigmatism, and coma. Tilt is a prismatic effect that produces either an image shift (for a point object), or a shape distortion (for an extended object). Astigmatism appears because the emerging refracted wavefront has two principal curvatures that determine two focal image points: the sagittal focus, where the sagittal (or horizontal) ray fan converges, and the tangential focus, where the tangential (or vertical) ray fan converges. The Sturm interval is defined as the difference between the sagittal and the tangential focal lengths, and it defines the amount of oblique astigmatism, which is the difference between the sagittal and tangential dioptric powers. Field curvature is a measure of defocus for off-axis objects and implies that the best image is formed not on the paraxial image plane but on a parabolic surface called the Petzval image surface (Smith & Atchison 1997). In real eyes, the retina, which may be approximated as a sphere with a radius between 11 and 13 mm, constitutes a curved image plane that in most cases compensates for field curvature. Thus, astigmatism and defocus have traditionally been assumed to be the main off-axis aberrations in the eye. This assumption has been validated with the use of new instruments to measure peripheral optics (Guirao & Artal 1999, Jaeken et al. 2011). **Figure 10** shows examples of wavefront aberrations at the fovea and at eccentricities of 30° in the nasal and temporal directions along the horizontal meridian (Jaeken &

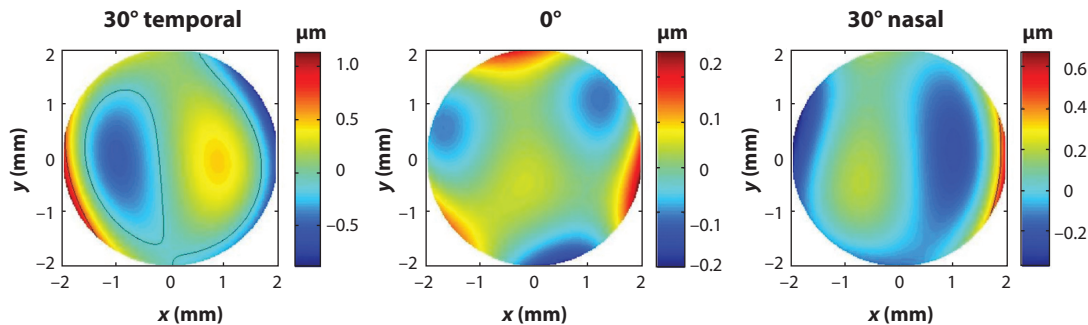


Figure 10

Examples of wavefront aberrations at the fovea and at 30° of eccentricity in the nasal and temporal directions along the horizontal meridian.

Artal 2012). One study (Lundström et al. 2007) has shown that in the periphery, the optics of the eye do not limit grating resolution. Or, equivalently, visual acuity in the periphery could not be improved with optical corrections. It is interesting to know, however, that our natural peripheral optics are also optimized by the gradient index structure of the crystalline lens. In a recent study (Jaeken et al. 2013), we compared the peripheral image quality in the eyes of a group of patients who had a monofocal intraocular lens implanted in one eye and an intact natural precataract lens in the fellow eye. The eyes with the implanted lenses had more astigmatism in the periphery than the normal eyes did. **Figure 11** shows the Strehl ratio (an image-quality parameter) as a function of eccentricity in eyes with a natural lens and in eyes with an artificial intraocular lens. The result depicted in this figure suggests that the crystalline lens provides a beneficial effect to partially compensate off-axis astigmatism, thereby improving peripheral optics.

INTRAOCULAR SCATTERING

Intraocular light scattering originates from localized irregularities of the refractive index within the ocular media and leads to the spread of light at large angles over the retina. This effect is usually described by the angular distribution of light intensity in the image plane. Aberrations and scatter are often treated separately, owing to their different origins, but they both contribute to the quality of the retinal image. **Figure 12** shows simulated retinal images of the moon depicting the contribution of each factor. Intraocular scattering has a significant impact on retinal image contrast for scenes containing a bright light source, such as those found in typical night driving. In general, scattered light reduces retinal image quality owing to a decrease in the contrast of the retinal images. The wide-angle PSF of the eye can provide a complete description of the optics, including aberrations and scattering. The aberrations largely determine the central part of the PSF (depicted as blur in the rightmost panel of **Figure 12a**), whereas the halo (the comparatively bright area in rightmost panel of **Figure 12b**) arises from scatter. There are some optical approaches for the direct measurement of the PSF using a double-pass measurement method in which a beam is directed into the eye and focused on the fundus by its optics. The aerial image after retinal reflection is then recorded by a camera (Santamaría et al. 1987). This technique measures the central part of the PSF, and its usefulness is usually limited for the eccentric areas owing to the dynamic range of the recording and to other possible artifacts. However, it can be applied in the case of eyes suffering from an elevated amount of scatter, such as those with cataracts (Artal et al. 2011). A new optical technique for the measurement of straylight by using extended

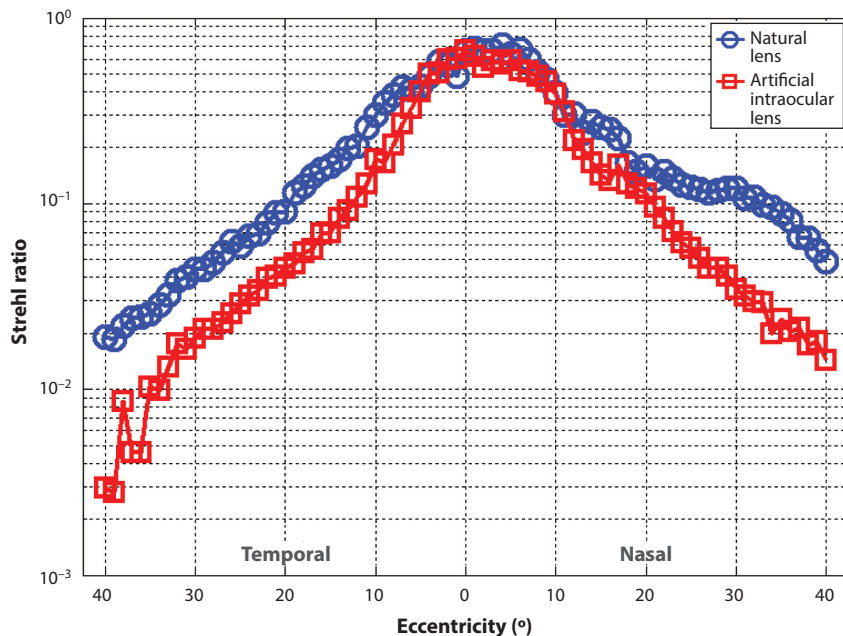


Figure 11

Image quality (quantified using the Strehl ratio) as a function of eccentricity in eyes with an intact natural lens (*blue circles*) and in eyes with an artificial intraocular lens (*red squares*).

a Aberrations



b Scattering



Figure 12

Simulated retinal images of the moon affected by (*a*) aberrations and (*b*) scattering.

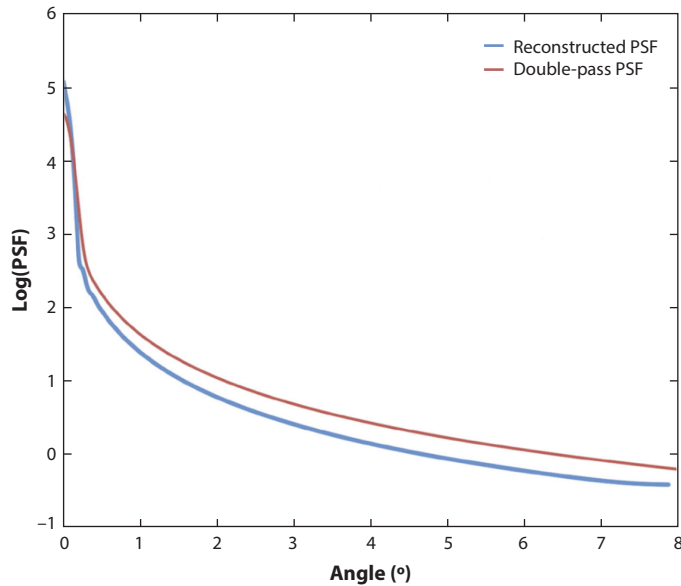


Figure 13

Plot showing two types of wide-angle point spread function (PSF) measurements for a normal eye.

sources and based on the optical integration method has also been developed (Ginis et al. 2012). In this method, a sequence of bright disks is projected onto the retinal fundus and imaged using a scheme that minimizes backscattering and specular reflections. The PSF can then be reconstructed from the recorded intensity at the center of each disk. This approach enhances the sensitivity of the double-pass technique and allows the PSF to be measured for angles of up to 8° and for different wavelengths (Ginis et al. 2013). **Figure 13** shows an example of the reconstructed and double-pass wide-angle PSFs measured in a normal young eye.

Possible interactions between aberrations and scattering may also affect vision. It has been shown (Pérez et al. 2009) that contrast sensitivity is reduced less by scattering when spherical aberration is present than when it is absent. This lack of reduction could be regarded as a compensatory mechanism, as, in the presence of scatter, the addition of spherical aberration under certain conditions could slightly improve image contrast. Although the visual effect observed was rather small, the combined presence of spherical aberration and scatter in the older eye could offer a mild protective effect, reducing the impact that each of the two factors might have on contrast vision separately. Note that the optics of the eye contain many other compensatory mechanisms that help to keep good vision during the life span. For example, although the aberrations of the eye increase with age, the average pupil diameter decreases, reducing their impact (Guirao et al. 1999).

SUMMARY POINTS

1. The wavelike nature of light and the properties of the eye combine to impose a first physical limit to vision.
2. The eye is not a centered optical system. The ocular surfaces are neither spherical in shape nor perfectly aligned, the fovea is decentered temporally, and the lens may be tilted and/or decentered with respect to the cornea.

3. Chromatic aberrations in the eye produce a difference of 2 diopters of defocus between blue and red objects, although this difference has a relatively small visual impact.
4. The optical system of the eye is optimized. The two main optical components, the cornea and the lens, have particular features that combine to improve the optical quality of the system.

DISCLOSURE STATEMENT

The author is not aware of any affiliations, memberships, funding, or financial holdings that might be perceived as affecting the objectivity of this review.

ACKNOWLEDGMENTS

Research supported by the Spanish Ministry of Science and Technology and the European Research Council.

LITERATURE CITED

- Artal P, Benito A, Pérez GM, Alcón E, De Casas A, et al. 2011. An objective scatter index based on double-pass retinal images of a point source to classify cataracts. *PLOS ONE* 6(2):e16823
- Artal P, Benito A, Tabernero J. 2006. The human eye is an example of robust optical design. *J. Vis.* 6:1–7
- Artal P, Berrio E, Guirao A, Piers P. 2002. Contribution of the cornea and internal surfaces to the change of ocular aberrations with age. *J. Opt. Soc. Am. A* 19:137–43
- Artal P, Chen L, Fernández EJ, Singer B, Manzanera S, Williams DR. 2004. Neural adaptation for the eye's optical aberrations. *J. Vis.* 4:281–87
- Artal P, Derrington AM, Colombo E. 1995. Refraction, aliasing, and the absence of motion reversals in peripheral vision. *Vis. Res.* 35:939–47
- Artal P, Ferro M, Miranda I, Navarro R. 1993. Effects of aging in retinal image quality. *J. Opt. Soc. Am. A* 10:1656–62
- Artal P, Guirao A, Berrio E, Williams DR. 2001. Compensation of corneal aberrations by internal optics in the human eye. *J. Vis.* 1:1–8
- Artal P, Manzanera S, Piers P, Weeber H. 2010. Visual effect of the combined correction of spherical and longitudinal chromatic aberrations. *Opt. Express* 18:1637–48
- Artal P, Navarro R. 1994. Monochromatic modulation transfer function of the human eye for different pupil diameters: an analytical expression. *J. Opt. Soc. Am. A* 11:246–49
- Artal P, Tabernero J. 2008. The eye's aplanatic answer. *Nat. Photonics* 2:586–89
- Atchison DA, Smith G. 2000. *Optics of the Human Eye*. Edinburgh, UK: Butterworth-Heinemann
- Bedford RE, Wyszecki G. 1957. Axial chromatic aberration of the human eye. *J. Opt. Soc. Am.* 47:564–65
- Benny Y, Manzanera S, Prieto PM, Ribak EN, Artal P. 2007. Wide-angle chromatic aberration corrector for the human eye. *J. Opt. Soc. Am. A* 24:1538–44
- Berrio E, Tabernero J, Artal P. 2010. Optical aberrations and alignment of the eye with age. *J. Vis.* 10:34
- Charman WN, Jennings JAN. 1976. Objective measurements of longitudinal chromatic aberration of human eye. *Vis. Res.* 16:999–1005
- Díaz JA, Irlbauer M, Martínez JA. 2004. Diffractive–refractive hybrid doublet to achromatize the human eye. *J. Mod. Opt.* 51:2223–34
- Ginis HS, Perez GM, Bueno JM, Artal P. 2012. The wide-angle point spread function of the human eye reconstructed by a new optical method. *J. Vis.* 12:20
- Ginis HS, Perez GM, Bueno JM, Pennos A, Artal P. 2013. Wavelength dependence of the ocular straylight. *Invest. Ophthalmol. Vis. Sci.* 54:3702–8

- Goodman JW. 2005. *Introduction to Fourier Optics*. Englewood, CO: Roberts & Co. 3rd ed.
- Guirao A, Artal P. 1999. Off-axis monochromatic aberrations estimated from double pass measurements in the human eye. *Vis. Res.* 39:207–17
- Guirao A, González C, Redondo M, Geraghty E, Norrby S, Artal P. 1999. Average optical performance of the human eye as a function of age in a normal population. *Investig. Ophthalmol. Vis. Sci.* 40:203–13
- Hammond BR Jr, Wooten BR, Snodderly DM. 1997. Individual variations in the spatial profile of human macular pigment. *J. Opt. Soc. Am. A* 14:1187–96
- He JC, Burns SA, Marcos S. 2000. Monochromatic aberrations in the accommodated human eye. *Vis. Res.* 40:41–48
- Howarth PA, Zhang XX, Bradley A, Still DL, Thibos LN. 1988. Does the chromatic aberration of the eye vary with age? *J. Opt. Soc. Am. A* 2:2087–92
- Jaeken B, Artal P. 2012. Optical quality of emmetropic and myopic eyes in the periphery measured with high-angular resolution. *Investig. Ophthalmol. Vis. Sci.* 53:3405–13
- Jaeken B, Lundström L, Artal P. 2011. Fast scanning peripheral wave-front sensor for the human eye. *Opt. Express* 19:7903–13
- Jaeken B, Mirabet S, Marín JM, Artal P. 2013. Comparison of the optical image quality in the periphery of phakic and pseudophakic eyes. *Investig. Ophthalmol. Vis. Sci.* 54:3594–99
- Kuroda T, Fujikado T, Maeda N, Oshika T, Hirohara Y, Mihashi T. 2002. Wavefront analysis in eyes with nuclear or cortical cataract. *Am. J. Ophthalmol.* 134:1–9
- Le Grand Y, El Hage SG. 1980. *Physiological Optics*. Berlin: Springer
- Lundström L, Manzanera S, Prieto PM, Ayala DB, Gorceix N, et al. 2007. Effect of optical correction and remaining aberrations on peripheral resolution acuity in the human eye. *Opt. Express* 15:12654–61
- Manzanera S, Canovas C, Prieto PM, Artal P. 2008. A wavelength tunable wavefront sensor for the human eye. *Opt. Express* 16:7748–55
- Manzanera S, Prieto PM, Benito A, Tabernero J, Artal. 2015. Location of achromatizing pupil position and first Purkinje reflection in a normal population. *Investig. Ophthalmol. Vis. Sci.* 56:962–66
- Maréchal A. 1947. Etude des effets combinés de la diffraction et des aberrations géométriques sur l'image d'un point lumineux. *Rev. Opt. Theor. Instrum.* 26:257–77
- Pedrotti FL, Pedrotti LS. 1993. *Introduction to Optics*. Englewood Cliffs, NJ: Prentice-Hall. 2nd ed.
- Pelli DG. 1990. The quantum efficiency of vision. In *Vision: Coding and Efficiency*, ed. C Blakemore, pp. 3–24. New York: Cambridge Univ. Press
- Pérez GM, Manzanera S, Artal P. 2009. Impact of scattering and spherical aberration in contrast sensitivity. *J. Vis.* 9:19
- Powell I. 1981. Lenses for correcting chromatic aberration of the eye. *Appl. Opt.* 20:4152–55
- Santamaría J, Artal P, Bescós J. 1987. Determination of the point-spread function of human eyes using a hybrid optical–digital method. *J. Opt. Soc. Am. A* 4:1109–14
- Schwarz C, Cánovas C, Manzanera S, Weeber H, Prieto PM, et al. 2014. Binocular visual acuity for the correction of spherical aberration in polychromatic and monochromatic light. *J. Vis.* 14:8
- Simonet P, Campbell MCW. 1990. The optical transverse chromatic aberration on the fovea of the human eye. *Vis. Res.* 30:187–206
- Smith G, Atchison DA. 1997. *The Eye and Visual Optical Instruments*. Cambridge, UK: Cambridge Univ. Press
- Tabernero J, Benito A, Alcón E, Artal P. 2007. Mechanism of compensation of aberrations in the human eye. *J. Opt. Soc. Am. A* 24:3274–83
- Tabernero J, Benito A, Nourrit V, Artal P. 2006. Instrument for measuring the misalignments of ocular surfaces. *Opt. Express* 14:10945–56
- Thibos LN, Bradley A, Still DL, Zhang X, Howarth PA. 1990. Theory and measurement of ocular chromatic aberration. *Vis. Res.* 3:33–49
- Thibos LN, Ye M, Zhang X, Bradley A. 1992. The chromatic eye: a new reduced-eye model of ocular chromatic aberration in humans. *Appl. Opt.* 31:3594–600
- van Norren D, Vos JJ. 1974. Spectral transmission of the human ocular media. *Vis. Res.* 14:1237–44
- Villegas EA, Alcón E, Artal P. 2008. Optical quality of the eye in subjects with normal and excellent visual acuity. *Investig. Ophthalmol. Vis. Sci.* 49:4688–96

- Villegas EA, Alcón E, Artal P. 2014. Minimum amount of astigmatism that should be corrected. *J. Cataract Refract. Surg.* 40:13–19
- Vinciguerra P, Albè E, Trazza S, Rosetta P, Vinciguerra R, et al. 2009. Refractive, topographic, tomographic, and aberrometric analysis of keratoconic eyes undergoing corneal cross-linking. *Ophthalmology* 116:369–78
- Wald G, Griffin DR. 1947. The change in refractive power of the human eye in dim and bright light. *J. Opt. Soc. Am.* 37:321–66
- Young T. 1801. On the mechanism of the eye. *Philos. Trans. R. Soc. Lond.* 91:23–88
- Zhang X, Bradley A, Thibos LN. 1991. Achromatizing the human eye: the problem of chromatic parallax. *J. Opt. Soc. Am. A* 8:686–91



Contents

An autobiographical article by Horace Barlow is available online at
www.annualreviews.org/r/horacebarlow.

Image Formation in the Living Human Eye <i>Pablo Artal</i>	1
Adaptive Optics Ophthalmoscopy <i>Austin Roorda and Jacque L. Duncan</i>	19
Imaging Glaucoma <i>Donald C. Hood</i>	51
What Does Genetics Tell Us About Age-Related Macular Degeneration? <i>Felix Grassmann, Thomas Ach, Caroline Brandl, Iris M. Heid, and Bernhard H.F. Weber</i>	73
Mitochondrial Genetics and Optic Neuropathy <i>Janey L. Wiggs</i>	97
Zebrafish Models of Retinal Disease <i>Brian A. Link and Ross F. Colclery</i>	125
Angiogenesis and Eye Disease <i>Yoshihiko Usui, Peter D. Westenskow, Salome Murinello, Michael I. Dorrell, Leah Schepke, Felicitas Bucher, Susumu Sakimoto, Liliana P. Paris, Edith Aguilar, and Martin Friedlander</i>	155
Optogenetic Approaches to Restoring Vision <i>Zhuo-Hua Pan, Qi Lu, Anding Bi, Alexander M. Dizhoor, and Gary W. Abrams</i>	185
The Determination of Rod and Cone Photoreceptor Fate <i>Constance L. Cepko</i>	211
Ribbon Synapses and Visual Processing in the Retina <i>Leon Lagnado and Frank Schmitz</i>	235
Functional Circuitry of the Retina <i>Jonathan B. Demb and Joshua H. Singer</i>	263

Contributions of Retinal Ganglion Cells to Subcortical Visual Processing and Behaviors <i>Onkar S. Dhande, Benjamin K. Stafford, Jung-Hwan A. Lim, and Andrew D. Huberman</i>	291
Organization of the Central Visual Pathways Following Field Defects Arising from Congenital, Inherited, and Acquired Eye Disease <i>Antony B. Morland</i>	329
Visual Functions of the Thalamus <i>W. Martin Usrey and Henry J. Alitto</i>	351
Neuronal Mechanisms of Visual Attention <i>John Maunsell</i>	373
A Revised Neural Framework for Face Processing <i>Brad Duchaine and Galit Yovel</i>	393
Deep Neural Networks: A New Framework for Modeling Biological Vision and Brain Information Processing <i>Nikolaus Kriegeskorte</i>	417
Visual Guidance of Smooth Pursuit Eye Movements <i>Stephen G. Lisberger</i>	447
Visuomotor Functions in the Frontal Lobe <i>Jeffrey D. Schall</i>	469
Control and Functions of Fixational Eye Movements <i>Michele Rucci and Martina Poletti</i>	499
Color and the Cone Mosaic <i>David H. Brainard</i>	519
Visual Adaptation <i>Michael A. Webster</i>	547
Development of Three-Dimensional Perception in Human Infants <i>Anthony M. Norcia and Holly E. Gerhard</i>	569

Errata

An online log of corrections to *Annual Review of Vision Science* articles may be found at
<http://www.annualreviews.org/errata/vision>